

Torsional stress analysis of the squirrel-cage rotor for three phase asynchronous motors

T Axinte¹ and C Nutu¹

¹Constanta Maritime University, Faculty of Naval Electro-Mechanics,
104 Mircea cel Batran Street, 900663, Constanta, Romania

E-mail: tibi_axinte@yahoo.com

Abstract. The paper aims to determine the torsional stress occurring in the rotor's shaft of the three phase asynchronous motors for a given rotational speed of the rotor. The three phase asynchronous motor is started using the main starting variants, each variant having its own torque characteristic which produces a certain maximum shear stress. The model uses several hypotheses regarding the geometry of the domain, the dynamic behavior, the friction phenomenon and the mass of the shaft which is disregarded in a model and it is considered in a more accurate model. The maximum shear stress is produced by the shock which occurs in the starting process of the motors. This maximum stress may lead to the failure of the rotor either because it breaks, or because of the fatigue of the material produced by frequent starting of the motor. Information resulted from this study are useful for the selection of the appropriate material, of the according geometry of the design and elaboration of the specifications for the in-service use of the motor. This theoretical study will be followed by the development of more accurate models which will also include experimental studies employed to calibrate the theoretical models and to verify their accuracy.

1. Introduction

The asynchronous electrical machines, also called three phase induction machines are the most frequently used alternative current electrical machines. The term “asynchronous” comes from the fact that the frequency of the stator field is slightly higher than the frequency of the rotor. These asynchronous machines can work both, as a generator and as well as motor. The main advantages of three-phase induction motors are the simplicity of their construction which induces advantageous cost prices and their safety in exploitation [1].



Figure 1. Three phase asynchronous electrical motor (induction motor).

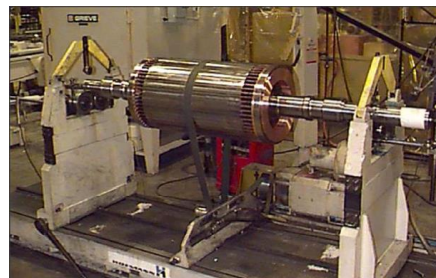


Figure 2. Rotor with two shafts.



One main characteristic of the induction motors is that their speed slightly reduces depending on increasing applied loads. That is why the asynchronous motors are generally used where the rotation speed must not vary with the applied load, such as for usual drilling, milling or hard machining mechanical tools, some of the lifting devices etc. [2].

- The main starting variants of the three phase asynchronous motors are:
- direct on-line start variant (DOL);
- the start variant using a star-delta connection, that is extensively used in practical conditions;
- the starting variant using a soft starter which is a modern, electronic alternative to star-delta starting variant for continuous and stepless motor start;
- the starting variant using a frequency inverter, that is the most expensive and modern variant, an important advantage being the fact that it enables a controlled, stepless motor start with rated load-torque.
- Each of the aforementioned starting methods has a certain torque characteristic and a certain relative starting torque determining a distinct torsional stress for each starting version.
- Among the main hypotheses we remind the most important ones, such as: the rotor's shaft has a cylindrical form of diameter D and moment of inertia J , and its steady state rotational speed is n .
- It is also assumed that the motor starts to rotate instantaneously with the angular speed ω . This means that the motor starts to rotate immediately, in this very short time being assumed that no heating due to the friction is produced. Therefore, the entire transmitted kinetic energy is transmitted to the rotor's shaft and transformed in strain energy.
- The maximum torsional stress in the shaft is produced by the shock conditions and they are calculated using two hypotheses. The first one takes into account the mass of the shaft and in the second hypothesis, the mass of the shaft being neglected.

The shock torsion produces high stresses which lead to the occurrence of cracks or even the shock breaking of the shaft. Moreover, the development of the cracks leads to the fatigue of the shafts' material.

2. Theoretical aspects

The following figures are presenting the ensemble induction motor-shaft-flywheel, viewed only from two different angles.

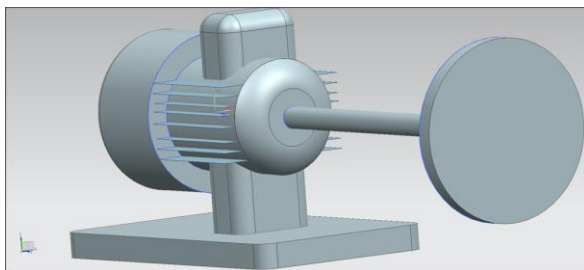


Figure 3. The assembly flywheel – left side – frontal view.

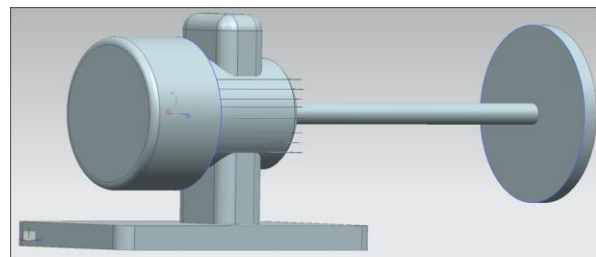


Figure 4. The assembly motor-shaft-flywheel: right motor-shaft-side – back view.

The working assumption used in the paper is that the whole amount of the kinetic energy of the flywheel is transmitted by means of deformation energy of the shaft.

Consequently we shall equal the amount of kinetic energy of the flywheel [3]:

$$W = \frac{1}{2} \cdot J \cdot \omega^2 \quad (1)$$

with the deformation energy of the shaft:

$$W = \int \frac{M_t^2}{2 \cdot G \cdot I_p} dx \quad (2)$$

In order to express this deformation energy of shaft depending on the shear stress τ_{\max} , at the end of the shaft's section, we use the following formulas, thus eliminating the value of torque, M_t from the deformation energy.

$$\tau_{\max} = \frac{M_t}{W_p} = \frac{M_t \cdot d}{2 \cdot I_p} \quad (3)$$

The twisting moment is

$$M_t = \frac{2 \cdot \tau_{\max} \cdot I_p}{d} \quad (4)$$

and the new form of the energy, [4], is

$$W = \frac{1}{2 \cdot G \cdot I_p} \int_0^l \left(\frac{2 \cdot \tau_{\max} \cdot I_p}{d} \right)^2 dx = \frac{2 \cdot \tau_{\max}^2 \cdot l}{G \cdot d^2} \quad (5)$$

In our case:

$$I_p = \frac{\pi \cdot d^4}{32} \quad (6)$$

and

$$\frac{\pi \cdot d^2}{4} l = V \quad (7)$$

It results:

$$W = \frac{2 \cdot \tau_{\max} \cdot \frac{\pi \cdot d^4}{32} \cdot l}{G \cdot d^2} = \frac{1}{2} \cdot \frac{\tau_{\max}}{2 \cdot G} \cdot V = \frac{\tau_{\max} \cdot V}{4 \cdot G} \quad (8)$$

By equating the both, kinetic and deformation energy

$$\frac{1}{2} \cdot J \cdot \omega^2 = \frac{\tau_{\max}^2}{4 \cdot G} \cdot V, \quad (9)$$

it results the maximum shear stress τ_{\max} :

$$\tau_{\max} = \omega \cdot \sqrt{\frac{2 \cdot J \cdot G}{V}} \quad (10),$$

with the formula of the moment of inertia, J , for a disk-shaped flywheel having the weight N :

$$J = \frac{N \cdot D^2}{8 \cdot g} \quad (11)$$

3. Results and discussions

Using many values N , of the weight of the disk-shaped flywheel with different diameters, as in the following table:

Table 1. The N and D values.

No	N	D
	[kg]	[cm]
1	10	20
2	15	25
3	20	30

```
>// If we have the following values:
>N = [10, 15,20]; // [kg]
>D = [20, 25, 30]; // [cm]
>g = 981; // [cm/s^2]
>// Determination of the mass moment of inertia of a disk-shaped flywheel diameter D;
>J = (N*D^2)/(8*981) // [kg*cm*s^2]
[0.509684, 1.19457, 2.29358]
```

Figure 5. Determination of the mass moment of inertia.

Supposing, in our case, that the diameter of the shaft is $d=5$ cm having the length, $l=3$ m, in the blocking moment of the flywheel, the rotation speed was $n=150$ rpm [5].

The corresponding angular speed is:

$$\omega = \frac{2 \cdot \pi \cdot n}{60} = \frac{2 \cdot \pi \cdot 150}{60} = 5\pi \quad [\text{rad/s}] \quad (12)$$

The volume is:

$$V = \frac{\pi \cdot d^2}{4} l = \frac{\pi \cdot 5^2 \cdot 300}{4} = 1875\pi \quad [\text{cm}^3] \quad (13)$$

The maximal shear stress for this flywheel can be determined:

```
>// Determination of the maximum shear stress of a disk-shaped flywheel diameter D:
>Tmax(1) = (((2*810000*246.49*J1)/5887.5)^(1/2))/(9.80665) // [N/cm^2]
[18.9593, 29.0253, 40.2187]
```

Figure 6. Determination of the maximum shear stress.

The shock-torsion phenomenon for shafts located between the motor and flywheel has been also studied using the finite element method and analysis, based on performant software.

As it can be seen also in the following drawings, the most torsion-stressed element is the shaft, the von Mises stresses at the flywheel, occurring only at the join between the shaft and flywheel.

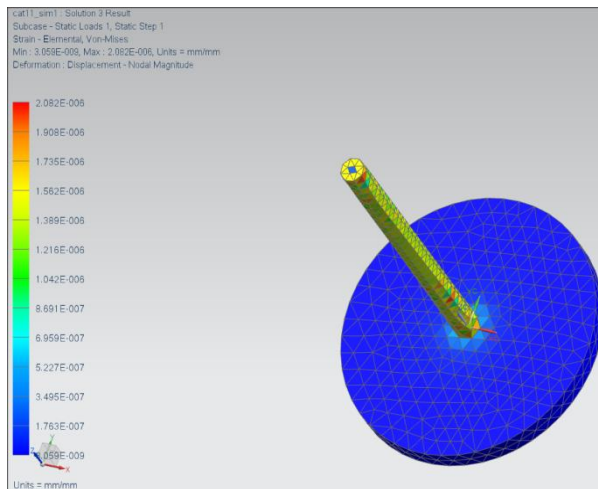


Figure 7. Shaft-flywheel assembly at a reduced torsional stress.

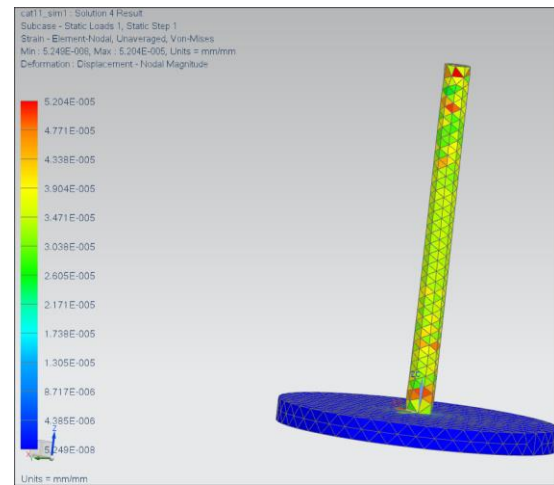


Figure 8. Shaft-flywheel assembly at a higher torsional stress.

Since the flywheel is considered to be as the part of a system that suddenly blocks, then the flywheel suddenly stops, as well.

As it is being shown and can be observed in figure 7 and figure 8, when suddenly halting the flywheel, the intuitive fact that can be remarked, is that the stresses do not occur on the surface of the flywheel, but only in the joint surfaces between the shaft and the flywheel. These stresses are being transmitted, further on, in the shaft body.

The formula used in the present paper for estimation of the maximal shear stress represents a good approximation of the maximal shear stress values occurring in fact, when the shaft-flywheel ensemble suddenly blocks. This simplified formula used is modeling the reality of the torsion phenomenon that occurs in the analyzed ensemble.

Analyzing this approximation and simplified used formula of the maximal shear stress, it results that the main factors determining the values of the maximal shear stresses (τ_{\max}) are to be controlled either by modifying the geometry and material of the studied ensemble, or by controlling the initial rotation speed of the ensemble, which is the speed of the motor used to drive the ensemble.

Thus, for certain geometry of the ensemble, this time driven by a rotation speed multiplied by a certain factor “n”, in order to obtain about the same value of the maximal shear stress (τ_{\max}), the material which has to be used in this second considered alternative, is to have a density which is of about n^2 times lesser than the density of the material initially used in the first alternative. Thus, the problem of the maximal shear stress occurring in a certain ensemble with different possible geometries becomes either a problem of the discipline of the strength of materials or a problem of the optimization of the geometry of the analyzed ensemble.

In practical engineering the problem of shear stresses is solved by treating these both problems and since the spectrum of the materials used is somehow both limited, at one hand by the materials presently known and on the other hand by their costs, the geometry of the ensemble is the easier part to be controlled by using appropriate software programs.

4. Conclusions

In practical conditions the effects of the shock torsion consist of non-uniform distributed shear stresses occurring on the body of the shaft, figure 7 and figure 8. These maximum shear stresses may produce the deformation and even breakage in some areas of the shaft.

Usually, under the torsional shock conditions the arm between the electrical motor and flywheel is the first which collapses. There are most uncommon cases when the rotor of the electrical motors breaks.

While for the second case, the result is consisting mainly in destroying only the electrical motor by its rotor's collapse, for the first case of arm failing, the entire ensemble (electrical machine, arm and flywheel) could be destroyed, as a result of the breakage.

In order to avoid this, the dimensioning of the shaft should be done always bearing in mind that the stresses occurred are to be minimal, thus calculating them considering the proper safety factors. The paper also provides some initial instruments for the assessment of the stresses in the flywheel-shaft-motor assembly that will be further on used for comparison with the results provided by the models to be developed using the Euler Math Toolbox software and Femap software.

The maximum stresses resulted from the study must be analyzed using the fatigue of materials theoretical background in order to minimize the risks in operating conditions. Moreover, by considering the factors which modify the endurance limit, such as: stress concentrators, size of the part, surface finishing, other miscellaneous influences, there may be conceived products with a longer life in service.

Another concern regards the shocks which may produce large contact stresses that are generating cracks and local high temperatures caused by friction and by the operating conditions. All these joined effects, together with the temperature in steady state conditions may lead to lower values of the material constants and ultimate stresses, the final effect being an early fail of the assembly. The worn supports may lead to vibrations which may also produce shock forces, leading to increased values of the stresses.

To conclude, the paper is an initial analysis which offers some insights regarding the basic phenomena occurring in the electric motor's assembly at this point being approached only from the point of view of the phenomena analytically modeled using the strength of materials theory. In this way, the paper presents a mechanical engineering application in the electrical engineering field.

The research will be continued with more accurate models which will take into account several aspects of the mechanical and electrical phenomena, specific to the electrical machines. The research will also include some experimental studies employed to calibrate the theoretical models and to verify the accuracy of their results. Therefore, it is possible to finally create a hybrid model which includes theoretical (analytical and numerical) aspects as well as experimental studies, [6].

References

- [1] *API 684* First Edition 1996 An Introduction to Lateral Critical and Train Torsional Analysis and Rotor Balancing
- [2] Fitzgerald A E, Kingsley C Jr and Umans S D 2004 *Electric Machinery* **6** (McGraw-Hill)
- [3] Buzdugan G 1970 *Rezistentă materialelor* (Bucharest: Tehnica Publishing House)
- [4] Voinea R et al. 1989 *Introducere în mecanica solidului cu aplicații în inginerie* (Romanian: Academy Publishing House)
- [5] Chiasson J 2005 *Modeling and High-Performance Control of Electric Machines* (online edition: Wiley)
- [6] Oanta E, Panait C, Axinte T and Dascalescu A E 2014 Instrumente software originale folosite ca interfețe în cadrul modelelor hibride din ingineria mecanică *AGIR* **4**